iScience

CellPress
OPEN ACCESS

Article

Myoglobin modulates the Hippo pathway to promote cardiomyocyte differentiation

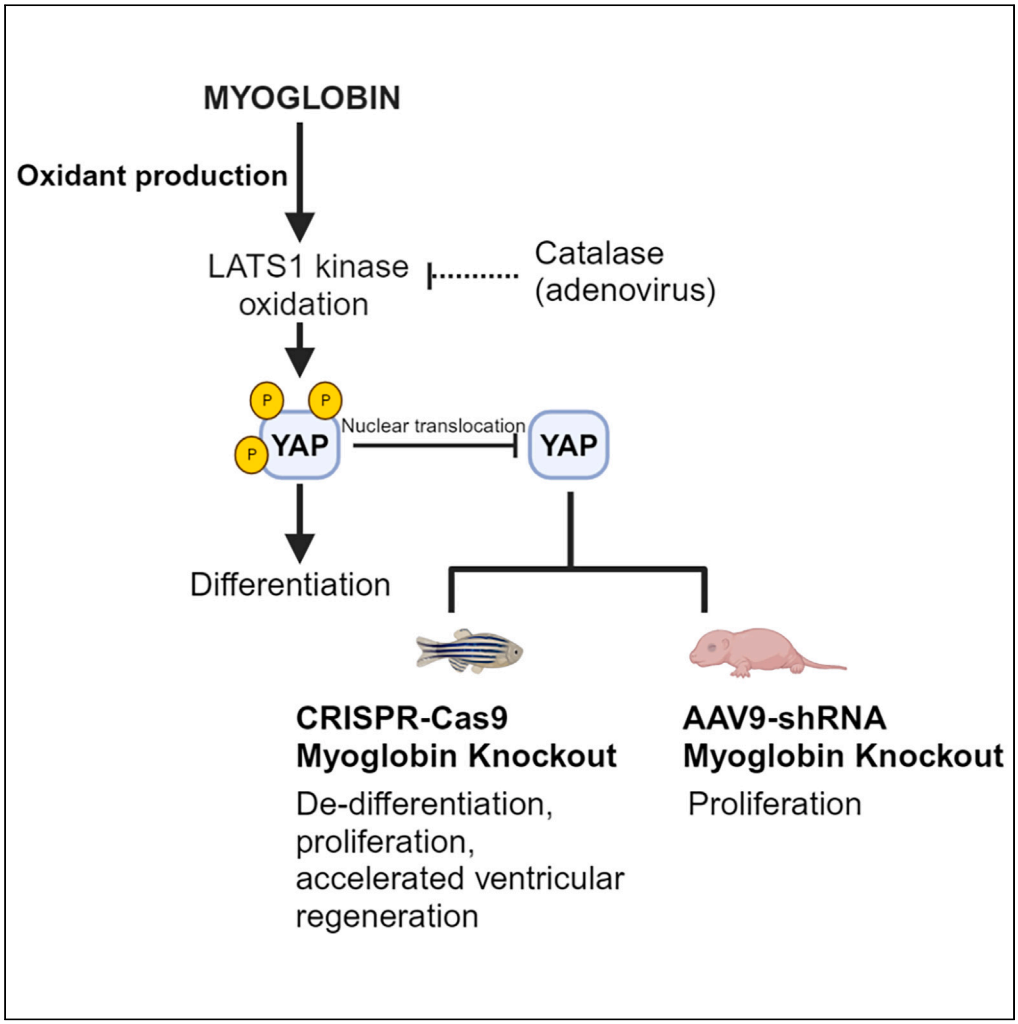

Krithika Rao, Elizabeth Rochon, Anuradha Singh, ..., Anita Saraf, Paola Corti, Sruti Shiva

sss43@pitt.edu

Highlights

Deletion of myoglobin represses gene expression of cardiomyocyte differentiation markers

Myoglobin's heme prosthetic group catalyzes oxidation and activation of LATS1 kinase

Deletion of myoglobin results in YAP activation and nuclear translocation

Myoglobin deletion causes cardiomyocyte cycling in zebrafish and neonatal mice

Rao et al., iScience 27, 109146
March 15, 2024
https://doi.org/10.1016/j.isci.2024.109146

iScience

CellPress
OPEN ACCESS

Article

Myoglobin modulates the Hippo pathway to promote cardiomyocyte differentiation

Krithika Rao,[1] Elizabeth Rochon,[1] Anuradha Singh,[1] Rajaganapathi Jagannathan,[1,3] Zishan Peng,[5] Haris Mansoor,[7] Bing Wang,[6] Mousumi Moulik,[1,3] Manling Zhang,[1,4,5] Anita Saraf,[7] Paola Corti,[1,5] and Sruti Shiva[1,2,8,*]

SUMMARY

The endogenous mechanisms that propagate cardiomyocyte differentiation and prevent de-differentiation remain unclear. While the expression of the heme protein myoglobin increases by over 50% during cardiomyocyte differentiation, a role for myoglobin in regulating cardiomyocyte differentiation has not been tested. Here, we show that deletion of myoglobin in cardiomyocyte models decreases the gene expression of differentiation markers and stimulates cellular proliferation, consistent with cardiomyocyte de-differentiation. Mechanistically, the heme prosthetic group of myoglobin catalyzes the oxidation of the Hippo pathway kinase LATS1, resulting in phosphorylation and inactivation of yes-associated protein (YAP). *In vivo*, myoglobin-deficient zebrafish hearts show YAP dephosphorylation and accelerated cardiac regeneration after apical injury. Similarly, myoglobin knockdown in neonatal murine hearts shows increased YAP dephosphorylation and cardiomyocyte cycling. These data demonstrate a novel role for myoglobin as an endogenous driver of cardiomyocyte differentiation and highlight myoglobin as a potential target to enhance cardiac development and improve cardiac repair and regeneration.

INTRODUCTION

The cardiomyocyte is the primary cell-type responsible for heart muscle contraction. In order to perform this highly specialized function, cardiomyocytes withdraw from the cell cycle soon after birth to become terminally differentiated.[1,2] Through the process of differentiation, they acquire the structural, functional, and metabolic characteristics necessary to power repeated contraction-relaxation cycles.[3] While fetal cardiomyocytes are proliferative, differentiated cardiomyocytes rarely re-enter the cell cycle (frequency <1%), in part due to their complex, well-organized cytoskeletal architecture.[4,5] A key feature of cardiomyocyte differentiation is the downregulation of fetal gene signatures including cell cycle markers, and upregulation of differentiation markers including mature sarcomeric genes such as *troponin*, *myosin light chain*, and *myosin heavy chain*.[6–8] Cardiomyocytes remain terminally differentiated over a lifetime, and loss of differentiation (i.e., de-differentiation) is associated with cellular remodeling in multiple pathological conditions.[9] While the markers and phenotypic features distinguishing differentiated from immature or de-differentiated cardiomyocytes are well-characterized, the endogenous mechanisms that drive and maintain differentiation or enable de-differentiation are not well-defined.

Myoglobin (Mb) is a monomeric heme protein constitutively expressed at high micromolar (200–300 μM) concentrations in cardiomyocytes.[10] The classic function of Mb in cardiomyocytes is considered to be oxygen storage and delivery to support mitochondrial respiration during hypoxia.[11,12] More recent studies have identified new roles for Mb in regulating tissue nitric oxide (NO) bioavailability and cellular reactive oxygen species (ROS) levels. Similar to the mechanism of oxygen storage and transport, these functions of Mb are dependent on the protein's heme prosthetic group. For example, oxidation of the ferric (Fe^{3+}) and ferrous (Fe^{2+}) forms of the heme center of Mb results in ferryl Mb ($MbFe^{4+}$), which, through its pseudo-peroxidase activity, can oxidize biomolecules such as nucleic acid, amino acids and lipids.[13,14,15] *In vivo*, Mb autooxidation under conditions of ischemia/reperfusion has been regarded as a significant source of oxidants that contributes to oxidative damage in the heart.[16,17] However, the contribution of Mb's oxidative signaling to physiological cardiomyocyte function is less well defined. Notably, during the developmental period of cardiac differentiation, the cardiac concentration of Mb increases by over 50% compared to the fetal heart.[18] Further, global Mb deletion causes embryonic lethality, and mice that do survive to adulthood encompass

[1]Heart, Lung, Blood Vascular Medicine Institute, University of Pittsburgh, Pittsburgh, PA 15261, USA
[2]Department of Pharmacology & Chemical Biology, University of Pittsburgh, Pittsburgh, PA 15261, USA
[3]Division of Cardiology, Department of Pediatrics, University of Pittsburgh, Pittsburgh, PA 15261, USA
[4]Division of Cardiology, Veteran Affair Pittsburgh Healthcare System, Pittsburgh, PA 15240, USA
[5]Division of Cardiology, Department of Medicine, University of Pittsburgh, Pittsburgh, PA 15213, USA
[6]Molecular Therapy Lab, Stem Cell Research Center, University of Pittsburgh School of Medicine, Pittsburgh, PA 15261, USA
[7]Heart and Vascular Institute Division of Cardiology, Department of Medicine and Pediatrics, University of Pittsburgh Medical Center, Pittsburgh, PA, USA
[8]Lead contact
*Correspondence: sss43@pitt.edu
https://doi.org/10.1016/j.isci.2024.109146

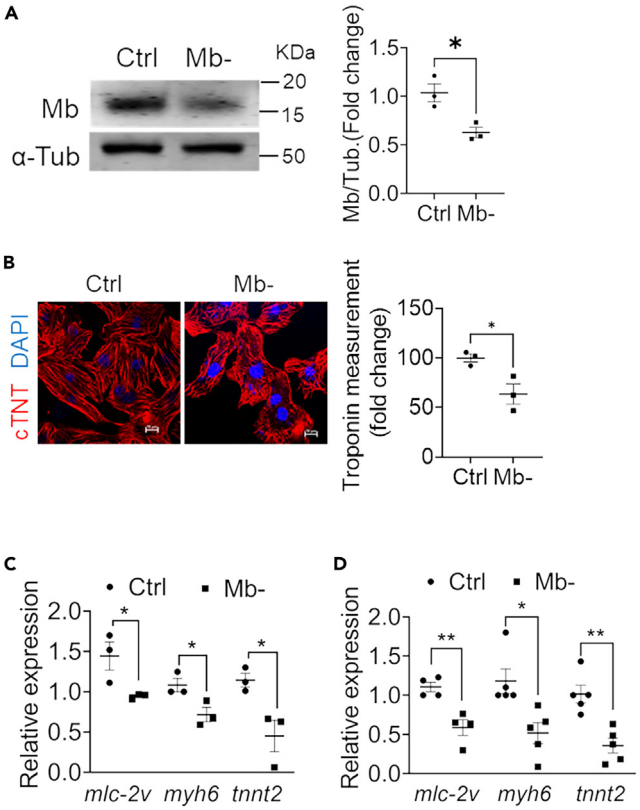

Figure 1. Deletion of endogenous myoglobin inhibits cardiomyocyte differentiation

(A) Representative western blot and quantification of Mb in NRVMs treated with control (Ctrl) or Mb targeted siRNA (Mb−). N = 3.

(B) Representative immunofluorescence images of NRVMs stained for cardiac troponin T (cTNT; red) to visualize sarcomeric structures and DAPI for nuclei (blue). Relative quantification of troponin fiber lengths in Mb− cells relative to control cells. Scale bar: 10 μm. N = 3.

(C) Relative mRNA expression of cardiac structural differentiation markers-m*lc-2v* (*myosin light chain*), *myh6* (*myosin heavy chain*), *tnnt2* (*cardiac troponinT*)- in NRVM compared to control undifferentiated cells after Mb knockdown. N = 3.

(D) Relative mRNA expression levels of cardiac structural differentiation markers in control and Mb− H9C2 cells. N = 4–5. Data are mean ± SEM; *p < 0.05, **p < 0.01.

multiple physiological compensatory adaptations for survival.[19–25] Despite the requirement for Mb and its dramatic increase in expression during cardiac development, the physiological role of Mb in cardiomyocyte differentiation has not been examined.

The Hippo signaling pathway maintains cardiomyocytes in a differentiated state by integrating extracellular cues with the activity of the transcriptional co-factor yes-associated protein (YAP).[26–28] YAP activity is propagated by its dephosphorylation and nuclear accumulation which potentiates a pro-proliferative and fetal gene transcription program. While the embryonic heart relies on YAP activity for proliferation, terminally differentiated cardiomyocytes predominantly express phosphorylated YAP (pYAP) which is sequestered in the cytoplasm for degradation. LATS1/2 is inactivation is sufficient to affect cardiomyocyte differentiation.[28,29] While recent discoveries reveal that signals outside of the canonical Hippo pathway can modify LATS1/2 activity, the effect of endogenous Mb and Mb-dependent signaling including the role of oxidants is unknown.[30–32]

In this study, we hypothesize that Mb regulates cardiomyocyte differentiation. We demonstrate that deletion of endogenous Mb prevents cardiomyocyte differentiation, resulting in the persistence of an undifferentiated, pro-proliferative phenotype. Mechanistically, we show that Mb oxidizes the Hippo Pathway enzyme LATS1 to increase its kinase activity and drive differentiation by YAP phosphorylation and inactivation. We demonstrate the activation of this pathway *in vivo* by first using a cardiac apical resection injury model in a mutant zebrafish line lacking Mb, in which we show that zebrafish lacking Mb have significantly accelerated scar regeneration post-injury; and secondly, in a murine model of cardiac myoglobin knockdown in which myoglobin deletion sustains cardiomyocyte YAP signaling and cellular proliferation. We discuss the potential implications of this Mb-dependent pathway in the context of understanding cardiac development as well as potential therapeutic strategies.

RESULTS

Endogenous myoglobin is required for differentiation

To determine whether endogenous Mb drives primary cardiomyocyte differentiation, we knocked down endogenous Mb using siRNA in isolated rat neonatal ventricular cardiomyocytes (NRVM; Figure 1A). Immunofluorescence staining for cardiac troponin T demonstrated that

NVRM lacking Mb (Mb− cells) were less successful at forming sarcomeric networks compared to control cells (Figure 1B) and had decreased expression of the structural markers *myosin light chain*, *beta-myosin heavy chain*, and *cardiac troponin-t* (Figure 1C). To enable mechanistic investigation of this effect, we utilized cultured H9C2 and HL-1 cells. Undifferentiated rat H9C2 myoblasts were transfected with siRNA targeting Mb (Figure S1A) and then stimulated with retinoic acid to stimulate differentiation. Mb-containing control cells differentiated to form morphologically characteristic multinucleated cells and expressed markers of structural differentiation including *myosin light chain*, *beta-myosin heavy chain*, and *cardiac troponin-t*, as well as those involved in the function of contractility and calcium signaling, while Mb deficient cells showed significantly lower levels of these markers (Figures 1D, S1B and S5B). A similar decrease in structural differentiation markers was observed in a differentiated HL-1 atrial cardiomyocyte cell line when Mb was knocked down (Figures S1C and S1D). siRNA mediated repression of Mb in differentiating iPSC cells starting at day 12 of differentiation prior to the onset of Mb expression (Figure S1E), inhibited expression of cardiomyocyte maturation markers by day 18 of differentiation (Figure S1F). Consistent with an undifferentiated state, NRVM, H9C2, and HL-1 cells lacking Mb proliferated at a higher rate compared to cells expressing endogenous Mb (Figures S2A–S2D) and expressed greater levels of the cell cycle drivers cyclin E and cyclin A and lower levels of the cell cycle inhibitor retinoblastoma protein (pRb) (Figure S2E). Taken together, these data demonstrate that endogenous Mb promotes and maintains cardiomyocyte differentiation.

Myoglobin promotes differentiation by YAP inactivation

We next sought to determine whether Mb promotes differentiation through the modulation of the Hippo pathway transcriptional co-activator YAP. Phosphorylation of YAP maintains the co-activator in an inactive state, while dephosphorylation activates YAP, enabling its nuclear translocation and transcriptional activity to drive cardiomyocyte proliferation and inhibit differentiation.[27,33] Knockdown of Mb in H9C2 cells significantly decreased the levels of pYAP at Ser127, a key phospho-site responsible for its inactivation, without changing total YAP (T-YAP) levels (Figure 2A). Notably, compared to overexpression of wild-type Mb, overexpression of an Mb mutant lacking the heme moiety (Apo-Mb) did not increase the levels of pYAP in H9C2 cells lacking endogenous Mb (Figure 2B). Mb deficient cells also demonstrated greater nuclear localization of YAP compared to controls treated with scrambled siRNA (Figure 2C). To test whether Mb-dependent phosphorylation altered YAP transcriptional activity, we transfected H9C2 control and Mb− cells with a luciferase reporter to measure the transcription of TEAD, a transcription factor that interacts with YAP. Consistent with YAP activation in cells lacking Mb, Mb− cells showed increased transcription of TEAD, confirming Mb knockdown increases YAP transcriptional activity (Figure 2D). Measurement of the mRNA levels of two classical gene targets of YAP, *ctgf* and *cyr61*, also showed higher levels in Mb deficient cells (Figure 2E), consistent with the TEAD reporter assay.

To test whether decreased YAP phosphorylation was responsible for the undifferentiated/proliferative phenotype observed with the deletion of Mb, we utilized a phospho-mimetic YAP mutant, YAP3D, which remains constitutively phosphorylated.[34] While Mb deficient cells had increased phospho-histone 3 levels indicating more proliferative activity as expected, overexpression of YAP3D in Mb− cells inhibited this increase (Figure S3A), demonstrating that Mb drives cellular differentiation through maintenance of YAP phosphorylation. Collectively, these results demonstrate that the loss of Mb decreases YAP phosphorylation, and enables its translocation to the nucleus, which results in a potentiation of its transcriptional activity. Further, this effect is dependent on the heme center of Mb.

Mb-derived ROS potentiates LATS1 kinase activity

To elucidate the mechanism by which Mb regulates YAP phosphorylation, we focused on LATS1/2, the upstream Hippo pathway kinase that phosphorylates YAP. LATS1 protein levels were not different between control and Mb deficient cells (Figure S3B). However, the kinase activity (the ability to phosphorylate YAP) of LATS1 in Mb deficient cells was significantly lower compared to LATS1 isolated from control cells (Figure 3A). In the canonical Hippo pathway, LATS1 activity is regulated by the upstream kinase MST1/2. However, the pharmacologic inhibition of MST1/2 (XMU-MP-1; 10 μM, 1 h)[35] inhibited LATS1 activity to the same extent in both control and Mb deficient cells (Figure S3C), precluding Mb-dependent regulation of MST1/2. Collectively these data suggest that Mb supports LATS1 kinase activity to increase YAP phosphorylation through a mechanism independent of MST1/2.

It is well established that kinase activity can be regulated by ROS and the heme moiety of Mb can catalyze the production of oxidants.[10,36] To test whether Mb-dependent hydrogen peroxide (H_2O_2) production modulates LATS1/YAP signaling, we first assessed cellular H_2O_2 production by control and Mb deficient cells. In accordance with prior studies,[36] Mb deficient cells generated lower levels of cellular H_2O_2 than control cells (Figure 3B). Furthermore, while overexpression of wild-type Mb in H9C2 cells lacking endogenous Mb increased cellular H_2O_2 levels, overexpression of Apo-Mb did not increase H_2O_2 production, demonstrating that Mb mediated H_2O_2 production is heme-dependent (Figure 3B).

To directly test whether Mb-dependent H_2O_2 regulates LATS1 activity, H9C2 cells were transduced with adenovirus to overexpress catalase (Figure S4A), which catalyzes the breakdown of H_2O_2. In Mb expressing cells, catalase overexpression decreased cellular H_2O_2 levels by ~50% as expected (Figure S4B). Catalase overexpression in control cells significantly decreased pYAP levels in Mb containing cells, (Figure 3C) and decreased the kinase activity of LATS1 (Figure 3D), mimicking the effect of Mb knockdown. Overexpression of catalase in control cells also inhibited the expression of the differentiation markers *mlc-2v* and *myh6* to the same extent as Mb deletion (Figure 3E).

Based on the observation that cellular ROS potentiated LATS1 activity, we tested whether LATS1 protein could be oxidatively modified. Utilizing an oxyblot assay, we measured Mb-dependent differential oxidative modifications of cellular proteins. Myoglobin-expressing control cells showed a higher level of oxidized LATS1 kinase compared to LATS1 kinase in Mb− cells (Figure S4C). Further, exposure of purified LATS1 active peptide to H_2O_2 significantly increased its kinase activity (Figure S4D). Collectively, these results demonstrate that Mb-dependent oxidation of LATS1 increases its kinase activity.

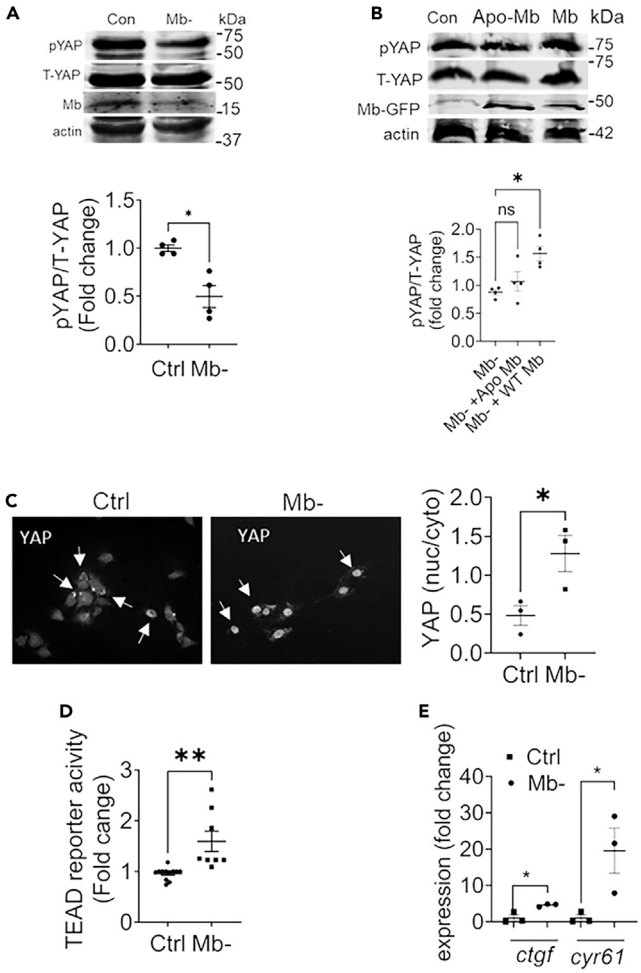

Figure 2. Myoglobin propagates YAP phosphorylation and inhibits its activity

(A) Representative western Blot and quantification of phospho-YAP (pYAP) and total YAP (T-YAP) in control and Mb− cells 48 h after knockdown, quantified as fold change of control; N = 4.

(B) Representative western blot and quantitation of pYAP and T-YAP levels in cells with Mb knockdown (control), followed by overexpression of Mb or Apo-Mb for 48 h using GFP tagged Mb or Apo-Mb plasmid. N = 4.

(C) Representative immunofluorescence images depicting YAP cellular localization in control and Mb− H9C2 cells. Arrows point to instance of cytoplasmic signal (Ctrl) and nuclear signal (Mb− image). Quantification is the ratio of nuclear to cytoplasmic staining intensity of YAP from 6 high-power field per sample; N = 3. Scale bar: 100 μm.

(D) TEAD-luciferase reporter signal in Mb− expressed as fold change of control cells; N = 3.

(E) Fold change over control in relative mRNA expression of YAP transcriptional target genes -*ctgf* and *cyr61*-in control and Mb− cells; N = 3. Data are mean ± SEM. *p < 0.05, **p < 0.01, n.s. = not significant.

Loss of Mb drives a pro-proliferative and regenerative response in zebrafish after cardiac injury

To determine whether Mb regulates YAP activity and cardiomyocyte proliferation *in vivo*, we generated mutant zebrafish deficient in Mb (*mb−/−*). We confirmed loss of Mb expression by immunofluorescence (Figure S5A) and western blot (Figure 4A). The fish developed normally and did not display any physiological phenotype. Consistent with our *in vitro* data, Mb deletion decreased the levels of pYAP in the zebrafish heart (Figure 4B). In zebrafish hearts, differentiated cardiomyocytes are able to regress to a de-differentiated state and subsequently proliferate in response to injury.[37] Thus, we employed a model of myocardial amputation in the zebrafish to test whether endogenous Mb regulates cardiomyocyte proliferation and heart regeneration. At 7 days following ventricular amputation, *mb−/−* hearts showed a significantly higher number of de-differentiated cardiomyocytes identified by staining for embryonic cardiac myosin heavy chain (embCMHC) (Figure 4C) and a higher number of proliferating cardiomyocytes compared to WT hearts (proliferation index 0.219 ± 0.057 in WT vs. 0.391 ± 0.128 in *mb−/−*) (Figure 4D).[38] To determine whether loss of Mb impacts long-term regeneration, we examined hearts for scar resolution using Acid Fuchsin Orange G (AFOG) staining. Zebrafish lacking Mb had significantly smaller scar area (4.07 ± 1.74%) at 20 days post amputation (dpa) compared to WT hearts (10.12 ± 5.92%). Notably, *mb−/−* zebrafish hearts showed no significant change in scar sizes between 20

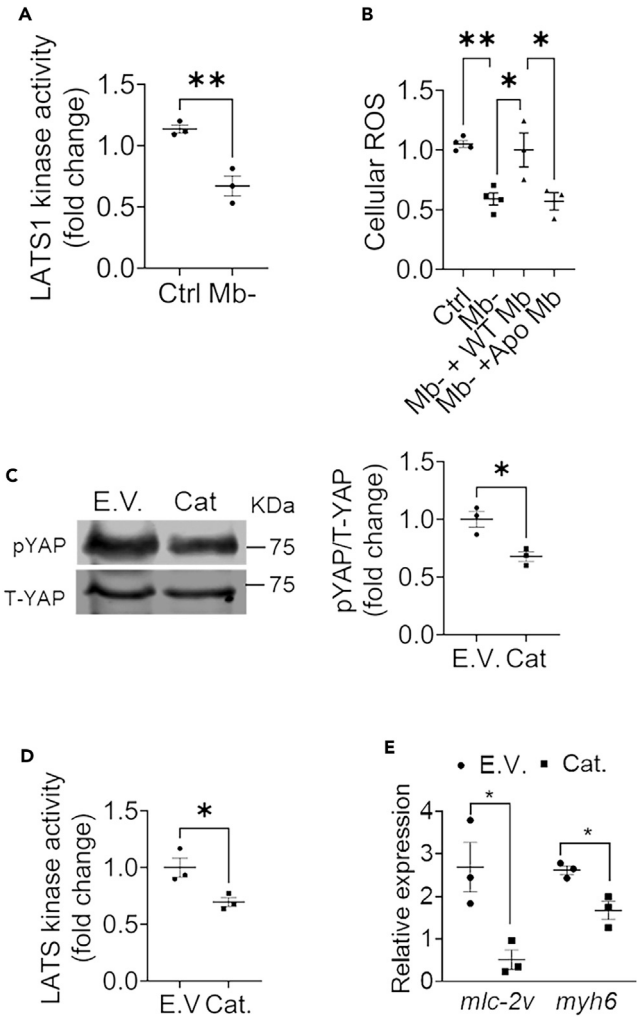

Figure 3. Scavenging H_2O_2 inhibits LATS1 activity

(A) LATS1 kinase activity of immunoprecipitated LATS1 from control and Mb− cells. N = 3.

(B) Cellular H_2O_2 levels in control, Mb−, Mb− cells with Mb overexpression and Apo-Mb overexpression; N = 3–4.

(C) Representative western blot and quantification for pYAP and T-YAP levels in H9C2 cells transduced with empty vector (Ad E.V.) or with adenoviral catalase (Ad Cat) expression; N = 3.

(D) LATS1 kinase activity in empty vector (Ad E.V.) or adenoviral catalase (Ad Cat) transduced H9C2 cells; N = 3.

(E) Relative expression of mRNA of cardiac differentiation markers in cells overexpressing empty vector control and catalase adenovirus compared with undifferentiated cells; N = 3. Data are mean ± SEM. *p < 0.05, **p < 0.01.

and 30 dpa, likely due to the fact that scarring was predominantly resolved at 20 dpa (Figure 4E).[37] These data demonstrate that Mb deficiency significantly increases cardiomyocyte proliferation and de-differentiation after injury, which potentiates rapid cardiac regeneration in this model.

Deletion of Mb inhibits YAP phosphorylation in the neonatal mouse heart

Murine cardiomyocytes are proliferative embryonically and have a short proliferative window until postnatal day 7, following which they exit the cell cycle.[1,39] We observed an increase in Mb expression in the heart as cardiomyocytes matured from the embryonic to adult stages of mouse development (Figure 5A). Correspondingly, there was a decrease in T-YAP and phospho-to-total YAP levels from the embryonic to adult stage (Figure 5A). To test the effect of Mb deletion on the Hippo pathway target YAP in postnatal mouse cardiomyocytes *in vivo*, we developed an AAV9 system to deliver shRNA targeting Mb to the mouse heart. Injection of AAV9 into postnatal day-1 old mice caused a significant (~50%) reduction in Mb levels and a decrease in pYAP by postnatal day 7 (Figure 5B). Further, the decrease in Mb caused a significant increase in the frequency of phospho histone 3 positive cardiomyocytes, indicative of more proliferation (Figure 5C).

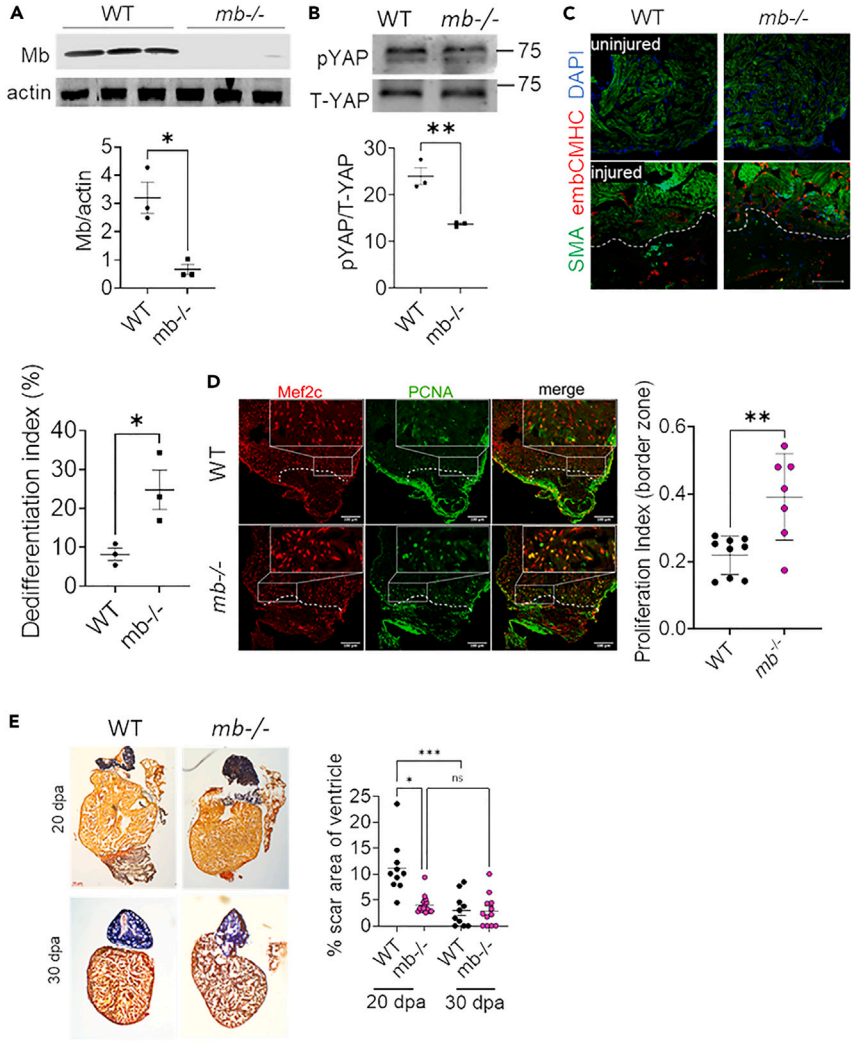

Figure 4. Loss of Mb promotes cardiomyocyte proliferation and regeneration *in vivo*

(A) Western blot and quantification of Mb in WT and *mb−/−* zebrafish hearts; N = 3 biological replicates.

(B) Representative western blot and quantification of pYAP and T-YAP WT and *mb−/−* zebrafish hearts; N = 3.

(C) Zebrafish heart section demonstrating the staining for de-differentiation marker embCMHC in red and α-sarcomeric actin in green at 7 days post amputation, and quantification of embCMHC cardiomyocytes (Differentiation index: % of cardiomyocytes expressing embCMHC in border zone of injury) from WT and *mb−/−* hearts; N = 3 from each group. Scale bar: 100 μm.

(D) Heart sections from WT and mb−/− zebrafish stained for Mef2c transcription factor (red) to identify cardiomyocytes and PCNA (green) to identify proliferating cells at 7 days post amputation: N = 7–9 individual zebrafish per group. Scale bar: 100 μm.

(E) Representative histological sections of AFOG stained tissue from WT and *mb−/−* zebrafish at 20- and 30-days post amputation stained to visualize fibrin (red), collagen (blue) and cardiac muscle (orange). Graph demonstrates the quantification of scar area on each section normalized to total ventricular area; N = 9–16 individual zebrafish per group. Scale bar: 100 μm. Data are mean ± SEM. *p < *0.05*, **p < 0.01, ****p < 0.0001.

DISCUSSION

The major finding of this study is that endogenous Mb expression propagates and maintains cardiomyocyte differentiation, and mechanistically, this is dependent on Mb-mediated oxidative regulation of the Hippo signaling pathway. Specifically, we show that Mb-dependent oxidation of LATS1 kinase potentiates its activity to phosphorylate and inactivate YAP, which inhibits its downstream transcriptional activity. Further, we show that this pathway is active *in vivo* as zebrafish lacking Mb show accelerated cardiac regeneration after injury. This study delineates a novel physiological role for Mb that has implications not only for cardiomyocyte maturation in cardiac development but also for potential regenerative therapeutic applications.

Our data suggest a fundamental physiological role for Mb in propagating and maintaining cardiomyocyte differentiation, distinct from its traditional function as an oxygen storage and delivery protein. While the role of Mb in driving oxidative stress has been examined in

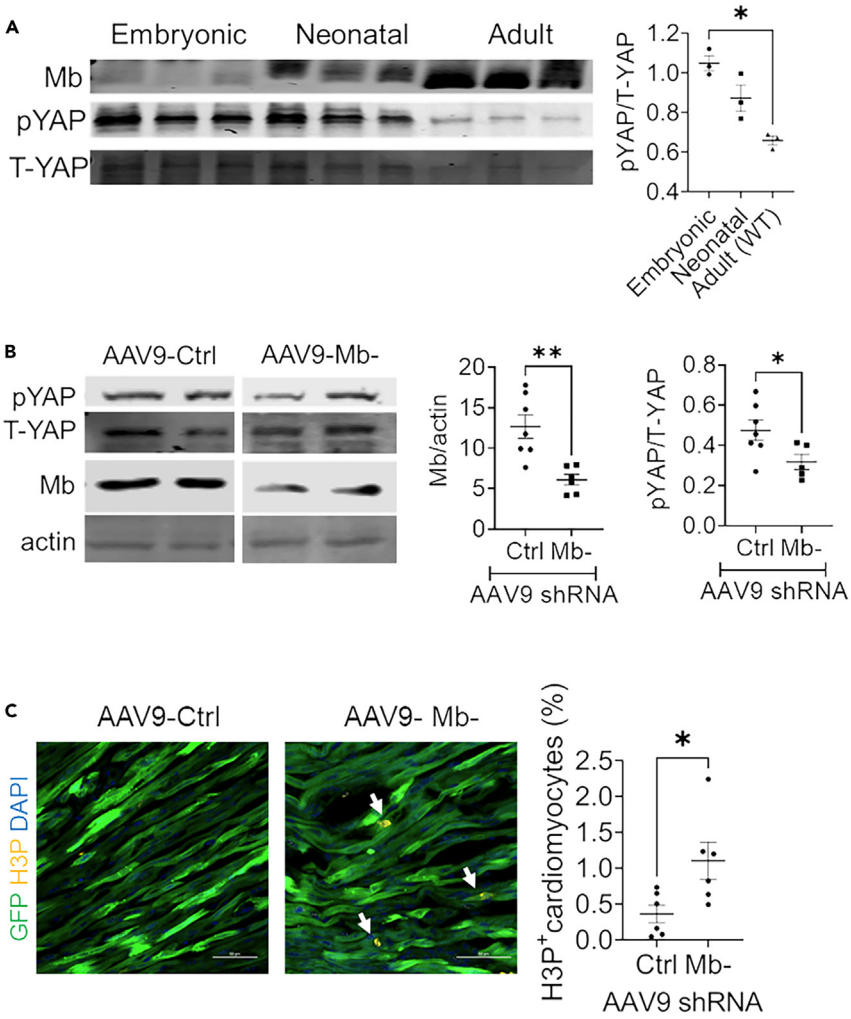

Figure 5. Deletion of Mb inhibits YAP phosphorylation in neonatal mouse hearts

(A) Western blot and relative quantification of pYAP to T-YAP ratios in embryonic (E14.5), fetal (postnatal day 3) and adult (10-week-old) mice. N = 3 mice per age.

(B) Representative western blot and relative quantification of pYAP to T-YAP ratios in postnatal day 7 mouse hearts after injection of AAV9 virus encoding a scramble control or Mb targeting shRNA into postnatal day 1 mice. N = 5–7 mice per group.

(C) Representative tissue sections and quantification of phospho histone 3 (H3P) staining from mice injected with control or Mb− targeted shRNA expressing AAV9. N = 6 mice per group. Arrow indicates $H3P^+$ nuclei and green represents the GFP cardiomyocytes infected with AAV9. Scale bar: 50 μm. Data are mean ± SEM. *p < *0.05*, **p < 0.01.

pathological contexts such myocardial infarction,[16] a physiological role for its oxidative signaling in cardiomyocytes has not been defined. Our data are consistent with an earlier report of H_2O_2 treatment inducing H9C2 cell-cycle arrest prior to differentiation, though the effect of this exogenous oxidant is more nuanced depending on timing and dose of exposure.[40] Importantly, the role of oxidants in cardiomyocyte maturation is established. Cellular ROS have been implicated in the mechanical or electrical stimuli-induced differentiation of embryonic cells to cardiomyocytes.[41–43] In contrast, scavenging or decreasing the levels of ROS using pyrrolidine dithiocarbamate, catalase, or N- acetylcysteine have been shown in other models to inhibit the formation of cardiomyocytes from developing embryoid bodies.[44] Despite their significance in cardiomyocyte differentiation, the endogenous source of ROS responsible for potentiation of differentiation remains less clear. Prior research has largely focused on the role of NADPH oxidases (NOX) enzymes as a source of intracellular oxidants in stimulating cardiomyocyte differentiation. Downregulation of NOX4 during early stages of cardio myogenesis inhibited cardiomyocyte differentiation.[43,44] The role of other sources of ROS are less clear. For example, conflicting studies demonstrate that ROS derived from mitochondria either stimulates or inhibits cardiomyocyte differentiation[45,46] and can also either induce cardiomyocyte cell-cycle arrest[39,47] or promote proliferation in the context of T3 signaling.[48,49] Our results demonstrate Mb as a major source of cardiomyocyte ROS which significantly impacts cardiomyocyte differentiation. It is established that the levels of Mb dynamically increase during development from the fetal to adult stage, and that this correlates with the development time period of increased cardiomyocyte differentiation.[18] However, how this change alters cardiac development is unknown.

Despite its significance in development, homeostasis and tissue repair, the endogenous mechanisms regulating the Hippo pathway and the phosphorylation of YAP in cardiomyocytes are yet to be completely uncovered.[50] The data herein demonstrate that Mb-mediated oxidative signaling is a critical regulator of the Hippo pathway that maintains YAP in its phosphorylated state. Prior studies utilizing exogenous oxidants, such as H_2O_2 have shown that the upstream kinase MST1 can be oxidatively modified and activated in a Prdx1 dependent manner.[51–53] While it is possible that Mb-dependent ROS can alter MST1 to alter LATS1 activity, our data with the MST1 inhibitor (XMU-MP-1) as well as with the purified LATS1 peptide suggest an additional mechanism of LATS1 regulation, independent of MST1. Our study thus extends the paradigm of oxidative activation of the Hippo kinase cascade from the MST1 kinase to LATS1 kinase. The identification of Mb as a regulator of YAP phosphorylation not only demonstrates an endogenous oxidative mechanism of regulation of Hippo signaling, but potentially links Hippo signaling to the oxygen sensing properties of Mb, enabling a more intricate Mb-dependent signaling axis in the regulation of development and tissue repair.

In cardiomyocytes, LATS1 and LATS2 have overlapping functions in phosphorylating YAP,[28] and while our studies are currently limited to LATS1 kinase, it does not exclude LATS2 modification in a similar mechanism. Future studies will examine the role of cellular oxidants on LATS1/2 activity across different cell types, given the conserved nature of the pathway in multiple organs.[28,54,55] Beyond cellular homeostasis, active Hippo signaling functions as a tumor suppression mechanism in multiple cell types, and dysregulation of this pathway or hyperactivation of its effector YAP are extensively associated with cancer progression. We and others have reported that certain epithelial cancers aberrantly express Mb.[36] Our results also demonstrated that expression of holo-Mb but not Apo-Mb significantly inhibited proliferation of breast epithelial cancer cells, confirming a role for Mb-derived oxidants in regulating cancer cell fate. Examining the role of Mb on Hippo signaling beyond cardiomyocytes has the potential to advance the field of tissue growth and repair in other areas, such as in the development of anti-cancer therapies.[56]

Elucidation of the Mb-LATS1-YAP pathway provides a roadmap to potential therapeutics for cardiac repair. *In vivo* apical resection of the heart in our zebrafish model provides proof-of-concept that that Mb deletion drives cardiomyocyte de-differentiation and proliferation. This observation is further supported by our results using AAV9 to specifically knockdown Mb in neonatal mice where the cardiomyocytes are under regulation of the Hippo pathway and demonstrate limited proliferation. Though a limitation of these studies is the use of zebrafish and neonatal mouse models, our data using these models, particularly AAV-mediated Mb knockdown, overcome the confounding effect of the compensatory adaptations during early development that have been previously observed in the global Mb knockout murine model. Further study is required to test the pathway in adult mammalian injury models and humans, these observations suggest that loss of Mb may be protective following cardiac injury. One study that potentially provides evidence to support this hypothesis is that in which global Mb knockout mice infused with isoproterenol for 14 days were protected from left ventricular dilation and development of heart failure compared to wildtype mice which expressed Mb.[21] Indeed, it is well-documented that following injuries such as myocardial infarction or in progressive cardiomyopathies, there is a downregulation of endogenous Mb expression in multiple species including humans.[57–59] However, whether this downregulation modifies the course of recovery has not been considered and our results bring this question to the forefront of the field. Beyond development and endogenous repair, our data also offer a new strategy to contribute to the field induced pluripotent cell (iPSC) technology, which offers a viable source of cardiomyocytes to replace damaged tissue and integrate with the spared myocardium. It is possible that modulation of Mb-dependent cardiomyocyte differentiation can be translated to optimize protocols for increasing efficiency of iPSCs.[60–62] While our data show that Mb can drive regenerative events via YAP,[26–29,62–65] future studies should focus on whether Mb can affect reparative processes beyond these pathways. The possible mechanisms include altered oxidative stress response,[66] cellular metabolism,[67,68] promoting expression of other fetal genes,[61,67,69,70] or altering the extracellular environment.[33,71–74] It is also interesting to speculate that Mb, through its more recently described chemistry with reactive nitrogen species or fatty acid binding,[11,75–84] could impact the functional properties of cardiomyocytes to impact regeneration.

In summary, we have described a novel pathway by which Mb regulates cardiomyocyte differentiation. We show that this occurs via Mb-dependent ROS which regulates YAP/LATS1 signaling. The loss of Mb is beneficial for cardiac regeneration, in part through promoting substantial cardiomyocyte de-differentiation. Taken together, these results have strong implications for the role of Mb in regulating Hippo signaling, and for advancing the understanding of cardiac function under physiological and pathological conditions.

Limitations of the study

Our study identifies an endogenous role for Mb in promoting murine cardiomyocyte differentiation in a normal heart. However, further studies are required to examine its function following acute or chronic heart injury. An additional limitation of this study is the lack of examination of Mb deletion in the adult heart.

STAR★METHODS

Detailed methods are provided in the online version of this paper and include the following:

- KEY RESOURCES TABLE
- RESOURCE AVAILABILITY
  - Lead contact
  - Materials availability
  - Data and code availability
- EXPERIMENTAL MODEL AND STUDY PARTICIPANT DETAILS
  - Animal studies

SUPPLEMENTAL INFORMATION

Supplemental information can be found online at https://doi.org/10.1016/j.isci.2024.109146.

ACKNOWLEDGMENTS

We would like to thank Jianmin Xu for her technical expertise contributed toward this work. We would like to thank Dr. Jixin Dong, Eppley Institute for Research in Cancer and Allied Diseases, University of Nebraska Medical Center for kindly sharing the YAP3D mutant with us. The N2.261 embCMHC antibody developed by Dr David R Soll, was obtained from the Developmental Studies Hybridoma Bank, created by the NICHD of the NIH and maintained at The University of Iowa, Department of Biology, Iowa City, IA 52242. E.R. was supported by an NIH T32 training grant HL110849 and funding from the Hemophilia Center of Western Pennsylvania. M.M. is funded by NIH R01 HL147946. P.C. was supported by a Scientist Development Grant from the AHA. M.Z. was supported by NIH grant K08HL157616. S.S. is supported by NIH R01 AG-072734-01A1 and the Hemophilia Center of Western Pennsylvania. (The content is solely the responsibility of the authors and does not necessarily represent the official views of the National Institutes of Health).

AUTHOR CONTRIBUTIONS

Conceptualization, K.R and S.S.; methodology, K.R., S.S., E.R., P.C., and B.W.; investigation, K.R., E.R., A.Singh, R.J., Z.P., and H.M.; writing – original draft, K.R. and S.S.; writing – review & editing, K.R., E.R., P.C., and S.S.; resources, B.W., M.M., M.Z., A.Saraf, P.C., and S.S.; funding acquisition, S.S.; supervision, S.S.

DECLARATION OF INTERESTS

The authors declare no competing interests.

Received: January 28, 2023
Revised: September 30, 2023
Accepted: February 1, 2024
Published: February 6, 2024

REFERENCES

1. Ahuja, P., Sdek, P., and MacLellan, W.R. (2007). Cardiac myocyte cell cycle control in development, disease, and regeneration. Physiol. Rev. *87*, 521–544. https://doi.org/10.1152/physrev.00032.2006.
2. Soonpaa, M.H., Kim, K.K., Pajak, L., Franklin, M., and Field, L.J. (1996). Cardiomyocyte DNA synthesis and binucleation during murine development. Am. J. Physiol. *271*, H2183-9. https://doi.org/10.1152/ajpheart.1996.271.5.H2183.
3. Guo, Y., and Pu, W.T. (2020). Cardiomyocyte Maturation: New Phase in Development. Circ. Res. *126*, 1086–1106. https://doi.org/10.1161/circresaha.119.315862.
4. Hirschy, A., Schatzmann, F., Ehler, E., and Perriard, J.C. (2006). Establishment of cardiac cytoarchitecture in the developing mouse heart. Dev. Biol. *289*, 430–441. https://doi.org/10.1016/j.ydbio.2005.10.046.
5. Ahuja, P., Perriard, E., Perriard, J.C., and Ehler, E. (2004). Sequential myofibrillar breakdown accompanies mitotic division of mammalian cardiomyocytes. J. Cell Sci. *117*, 3295–3306. https://doi.org/10.1242/jcs.01159.
6. Siedner, S., Krüger, M., Schroeter, M., Metzler, D., Roell, W., Fleischmann, B.K., Hescheler, J., Pfitzer, G., and Stehle, R. (2003). Developmental changes in contractility and sarcomeric proteins from the early embryonic to the adult stage in the mouse heart. J. Physiol. *548*, 493–505. https://doi.org/10.1113/jphysiol.2002.036509.
7. Paige, S.L., Plonowska, K., Xu, A., and Wu, S.M. (2015). Molecular regulation of cardiomyocyte differentiation. Circ. Res. *116*, 341–353. https://doi.org/10.1161/circresaha.116.302752.

8. Cui, M., Wang, Z., Bassel-Duby, R., and Olson, E.N. (2018). Genetic and Epigenetic Regulation of Cardiomyocytes in Development, Regeneration and Disease. Development *145*. https://doi.org/10.1242/dev.171983.
9. Szibor, M., Pöling, J., Warnecke, H., Kubin, T., and Braun, T. (2014). Remodeling and dedifferentiation of adult cardiomyocytes during disease and regeneration. Cell. Mol. Life Sci. *71*, 1907–1916. https://doi.org/10.1007/s00018-013-1535-6.
10. Kamga, C., Krishnamurthy, S., and Shiva, S. (2012). Myoglobin and mitochondria: a relationship bound by oxygen and nitric oxide. Nitric Oxide. *26*, 251–258. https://doi.org/10.1016/j.niox.2012.03.005.
11. Wittenberg, B.A., and Wittenberg, J.B. (1987). Myoglobin-mediated oxygen delivery to mitochondria of isolated cardiac myocytes. Proc. Natl. Acad. Sci. USA *84*, 7503–7507. https://doi.org/10.1073/pnas.84.21.7503.
12. Wittenberg, B.A., Wittenberg, J.B., and Caldwell, P.R. (1975). Role of myoglobin in the oxygen supply to red skeletal muscle. J. Biol. Chem. *250*, 9038–9043.
13. Rao, S.I., Wilks, A., Hamberg, M., and Ortiz de Montellano, P.R. (1994). The lipoxygenase activity of myoglobin. Oxidation of linoleic acid by the ferryl oxygen rather than protein radical. J. Biol. Chem. *269*, 7210–7216.
14. Alayash, A.I., Patel, R.P., and Cashon, R.E. (2001). Redox reactions of hemoglobin and myoglobin: biological and toxicological implications. Antioxid Redox Signal *3*, 313–327. https://doi.org/10.1089/152308601300185250.
15. Giulivi, C., and Cadenas, E. (1998). Heme protein radicals: formation, fate, and biological consequences. Free Radic. Biol. Med. *24*, 269–279. https://doi.org/10.1016/s0891-5849(97)00226-8.
16. Gunther, M.R., Sampath, V., and Caughey, W.S. (1999). Potential roles of myoglobin autoxidation in myocardial ischemia-reperfusion injury. Free Radic. Biol. Med. *26*, 1388–1395. https://doi.org/10.1016/s0891-5849(98)00338-4.
17. Sylvén, C., Jansson, E., and Böök, K. (1984). Myoglobin content in human skeletal muscle and myocardium: relation to fibre size and oxidative capacity. Cardiovasc. Res. *18*, 443–446. https://doi.org/10.1093/cvr/18.7.443.
18. Longo, L.D., Koos, B.J., and Power, G.G. (1973). Fetal myoglobin: quantitative determination and importance for oxygenation. Am. J. Physiol. *224*, 1032–1036. https://doi.org/10.1152/ajplegacy.1973.224.5.1032.
19. Flögel, U., Laussmann, T., Gödecke, A., Abanador, N., Schäfers, M., Fingas, C.D., Metzger, S., Levkau, B., Jacoby, C., and Schrader, J. (2005). Lack of myoglobin causes a switch in cardiac substrate selection. Circ. Res. *96*, e68–e7575. https://doi.org/10.1161/01.RES.0000165481.36288.d2.
20. Park, J.W., Piknova, B., Dey, S., Noguchi, C.T., and Schechter, A.N. (2019). Compensatory mechanisms in myoglobin deficient mice preserve NO homeostasis. Nitric Oxide. *90*, 10–14. https://doi.org/10.1016/j.niox.2019.06.001.
21. Molojavyi, A., Lindecke, A., Raupach, A., Moellendorf, S., Köhrer, K., and Gödecke, A. (2010). Myoglobin-deficient mice activate a distinct cardiac gene expression program in response to isoproterenol-induced hypertrophy. Physiol. Genom. *41*, 137–145. https://doi.org/10.1152/physiolgenomics.90297.2008.
22. Meeson, A.P., Radford, N., Shelton, J.M., Mammen, P.P., DiMaio, J.M., Hutcheson, K., Kong, Y., Elterman, J., Williams, R.S., and Garry, D.J. (2001). Adaptive mechanisms that preserve cardiac function in mice without myoglobin. Circ. Res. *88*, 713–720. https://doi.org/10.1161/hh0701.089753.
23. Schlieper, G., Kim, J.H., Molojavyi, A., Jacoby, C., Laussmann, T., Flögel, U., Gödecke, A., and Schrader, J. (2004). Adaptation of the myoglobin knockout mouse to hypoxic stress. Am. J. Physiol. Regul. Integr. Comp. Physiol. *286*, R786–R792792. https://doi.org/10.1152/ajpregu.00043.2003.
24. Garry, D.J., Ordway, G.A., Lorenz, J.N., Radford, N.B., Chin, E.R., Grange, R.W., Bassel-Duby, R., and Williams, R.S. (1998). Mice without myoglobin. Nature *395*, 905–908. https://doi.org/10.1038/27681.
25. Gödecke, A., Flögel, U., Zanger, K., Ding, Z., Hirchenhain, J., Decking, U.K., and Schrader, J. (1999). Disruption of myoglobin in mice induces multiple compensatory mechanisms. Proc. Natl. Acad. Sci. USA *96*, 10495–10500. https://doi.org/10.1073/pnas.96.18.10495.
26. Xin, M., Kim, Y., Sutherland, L.B., Qi, X., McAnally, J., Schwartz, R.J., Richardson, J.A., Bassel-Duby, R., and Olson, E.N. (2011). Regulation of insulin-like growth factor signaling by Yap governs cardiomyocyte proliferation and embryonic heart size. Sci. Signal. *4*, ra70. https://doi.org/10.1126/scisignal.2002278.
27. von Gise, A., Lin, Z., Schlegelmilch, K., Honor, L.B., Pan, G.M., Buck, J.N., Ma, Q., Ishiwata, T., Zhou, B., Camargo, F.D., and Pu, W.T. (2012). YAP1, the nuclear target of Hippo signaling, stimulates heart growth through cardiomyocyte proliferation but not hypertrophy. Proc. Natl. Acad. Sci. USA *109*, 2394–2399. https://doi.org/10.1073/pnas.1116136109.
28. Heallen, T., Zhang, M., Wang, J., Bonilla-Claudio, M., Klysik, E., Johnson, R.L., and Martin, J.F. (2011). Hippo pathway inhibits Wnt signaling to restrain cardiomyocyte proliferation and heart size. Science *332*, 458–461. https://doi.org/10.1126/science.1199010.
29. Kastan, N., Gnedeva, K., Alisch, T., Petelski, A.A., Huggins, D.J., Chiaravalli, J., Aharanov, A., Shakked, A., Tzahor, E., Nagiel, A., et al. (2021). Small-molecule inhibition of Lats kinases may promote Yap-dependent proliferation in postmitotic mammalian tissues. Nat. Commun. *12*, 3100. https://doi.org/10.1038/s41467-021-23395-3.
30. Zou, J., Ma, W., Li, J., Littlejohn, R., Zhou, H., Kim, I.M., Fulton, D.J.R., Chen, W., Weintraub, N.L., Zhou, J., and Su, H. (2018). Neddylation mediates ventricular chamber maturation through repression of Hippo signaling. Proc. Natl. Acad. Sci. USA *115*, E4101–E4110. https://doi.org/10.1073/pnas.1719309115.
31. Kim, E., Kang, J.G., Kang, M.J., Park, J.H., Kim, Y.J., Kweon, T.H., Lee, H.W., Jho, E.H., Lee, Y.H., Kim, S.I., et al. (2020). O-GlcNAcylation on LATS2 disrupts the Hippo pathway by inhibiting its activity. Proc. Natl. Acad. Sci. USA *117*, 14259–14269. https://doi.org/10.1073/pnas.1913469117.
32. He, M., Zhou, Z., Shah, A.A., Hong, Y., Chen, Q., and Wan, Y. (2016). New insights into posttranslational modifications of Hippo pathway in carcinogenesis and therapeutics. Cell Div. *11*, 4. https://doi.org/10.1186/s13008-016-0013-6.
33. Xiao, Y., Hill, M.C., Zhang, M., Martin, T.J., Morikawa, Y., Wang, S., Moise, A.R., Wythe, J.D., and Martin, J.F. (2018). Hippo Signaling Plays an Essential Role in Cell State Transitions during Cardiac Fibroblast Development. Dev. Cell *45*, 153–169.e6. https://doi.org/10.1016/j.devcel.2018.03.019.
34. Yang, S., Zhang, L., Liu, M., Chong, R., Ding, S.J., Chen, Y., and Dong, J. (2013). CDK1 phosphorylation of YAP promotes mitotic defects and cell motility and is essential for neoplastic transformation. Cancer Res. *73*, 6722–6733. https://doi.org/10.1158/0008-5472.Can-13-2049.
35. Fan, F., He, Z., Kong, L.L., Chen, Q., Yuan, Q., Zhang, S., Ye, J., Liu, H., Sun, X., Geng, J., et al. (2016). Pharmacological targeting of kinases MST1 and MST2 augments tissue repair and regeneration. Sci. Transl. Med. *8*, 352ra108. https://doi.org/10.1126/scitranslmed.aaf2304.
36. Braganza, A., Quesnelle, K., Bickta, J., Reyes, C., Wang, Y., Jessup, M., St Croix, C., Arlotti, J., Singh, S.V., and Shiva, S. (2019). Myoglobin induces mitochondrial fusion, thereby inhibiting breast cancer cell proliferation. J. Biol. Chem. *294*, 7269–7282. https://doi.org/10.1074/jbc.RA118.006673.
37. Jopling, C., Sleep, E., Raya, M., Martí, M., Raya, A., and Izpisúa Belmonte, J.C. (2010). Zebrafish heart regeneration occurs by cardiomyocyte dedifferentiation and proliferation. Nature *464*, 606–609. https://doi.org/10.1038/nature08899.
38. Sallin, P., de Preux Charles, A.S., Duruz, V., Pfefferli, C., and Jaźwińska, A. (2015). A dual epimorphic and compensatory mode of heart regeneration in zebrafish. Dev. Biol. *399*, 27–40. https://doi.org/10.1016/j.ydbio.2014.12.002.
39. Puente, B.N., Kimura, W., Muralidhar, S.A., Moon, J., Amatruda, J.F., Phelps, K.L., Grinsfelder, D., Rothermel, B.A., Chen, R., Garcia, J.A., et al. (2014). The oxygen-rich postnatal environment induces cardiomyocyte cell-cycle arrest through DNA damage response. Cell *157*, 565–579. https://doi.org/10.1016/j.cell.2014.03.032.
40. Oyama, K., Takahashi, K., and Sakurai, K. (2011). Hydrogen peroxide induces cell cycle arrest in cardiomyoblast H9c2 cells, which is related to hypertrophy. Biol. Pharm. Bull. *34*, 501–506. https://doi.org/10.1248/bpb.34.501.
41. Sauer, H., Rahimi, G., Hescheler, J., and Wartenberg, M. (1999). Effects of electrical fields on cardiomyocyte differentiation of embryonic stem cells. J. Cell. Biochem. *75*, 710–723. https://doi.org/10.1002/(sici)1097-4644(19991215)75:4<710::aid-jcb16>3.0.co;2-z.
42. Serena, E., Figallo, E., Tandon, N., Cannizzaro, C., Gerecht, S., Elvassore, N., and Vunjak-Novakovic, G. (2009). Electrical stimulation of human embryonic stem cells: cardiac differentiation and the generation of reactive oxygen species. Exp. Cell Res. *315*, 3611–3619. https://doi.org/10.1016/j.yexcr.2009.08.015.

43. Schmelter, M., Ateghang, B., Helmig, S., Wartenberg, M., and Sauer, H. (2006). Embryonic stem cells utilize reactive oxygen species as transducers of mechanical strain-induced cardiovascular differentiation. FASEB J. *20*, 1182–1184. https://doi.org/10.1096/fj.05-4723fje.

44. Li, J., Stouffs, M., Serrander, L., Banfi, B., Bettiol, E., Charnay, Y., Steger, K., Krause, K.H., and Jaconi, M.E. (2006). The NADPH oxidase NOX4 drives cardiac differentiation: Role in regulating cardiac transcription factors and MAP kinase activation. Mol. Biol. Cell *17*, 3978–3988. https://doi.org/10.1091/mbc.e05-06-0532.

45. Birket, M.J., Casini, S., Kosmidis, G., Elliott, D.A., Gerencser, A.A., Baartscheer, A., Schumacher, C., Mastroberardino, P.G., Elefanty, A.G., Stanley, E.G., and Mummery, C.L. (2013). PGC-1α and reactive oxygen species regulate human embryonic stem cell-derived cardiomyocyte function. Stem Cell Rep. *1*, 560–574. https://doi.org/10.1016/j.stemcr.2013.11.008.

46. Hom, J.R., Quintanilla, R.A., Hoffman, D.L., de Mesy Bentley, K.L., Molkentin, J.D., Sheu, S.S., and Porter, G.A., Jr. (2011). The permeability transition pore controls cardiac mitochondrial maturation and myocyte differentiation. Dev. Cell *21*, 469–478. https://doi.org/10.1016/j.devcel.2011.08.008.

47. Zhang, D., Li, Y., Heims-Waldron, D., Bezzerides, V., Guatimosim, S., Guo, Y., Gu, F., Zhou, P., Lin, Z., Ma, Q., et al. (2018). Mitochondrial Cardiomyopathy Caused by Elevated Reactive Oxygen Species and Impaired Cardiomyocyte Proliferation. Circ. Res. *122*, 74–87. https://doi.org/10.1161/circresaha.117.311349.

48. Tan, L., Bogush, N., Naib, H., Perry, J., Calvert, J.W., Martin, D.I.K., Graham, R.M., Naqvi, N., and Husain, A. (2019). Redox activation of JNK2α2 mediates thyroid hormone-stimulated proliferation of neonatal murine cardiomyocytes. Sci. Rep. *9*, 17731. https://doi.org/10.1038/s41598-019-53705-1.

49. Murray, T.V.A., Smyrnias, I., Schnelle, M., Mistry, R.K., Zhang, M., Beretta, M., Martin, D., Anilkumar, N., de Silva, S.M., Shah, A.M., and Brewer, A.C. (2015). Redox regulation of cardiomyocyte cell cycling via an ERK1/2 and c-Myc-dependent activation of cyclin D2 transcription. J. Mol. Cell. Cardiol. *79*, 54–68. https://doi.org/10.1016/j.yjmcc.2014.10.017.

50. Wang, J., Liu, S., Heallen, T., and Martin, J.F. (2018). The Hippo pathway in the heart: pivotal roles in development, disease, and regeneration. Nat. Rev. Cardiol. *15*, 672–684. https://doi.org/10.1038/s41569-018-0063-3.

51. Rawat, S.J., Creasy, C.L., Peterson, J.R., and Chernoff, J. (2013). The tumor suppressor Mst1 promotes changes in the cellular redox state by phosphorylation and inactivation of peroxiredoxin-1 protein. J. Biol. Chem. *288*, 8762–8771. https://doi.org/10.1074/jbc.M112.414524.

52. Morinaka, A., Funato, Y., Uesugi, K., and Miki, H. (2011). Oligomeric peroxiredoxin-I is an essential intermediate for p53 to activate MST1 kinase and apoptosis. Oncogene *30*, 4208–4218. https://doi.org/10.1038/onc.2011.139.

53. Radu, M., and Chernoff, J. (2009). The DeMSTification of mammalian Ste20 kinases. Curr. Biol. *19*, R421–R425. https://doi.org/10.1016/j.cub.2009.04.022.

54. Zhao, B., Li, L., Lei, Q., and Guan, K.L. (2010). The Hippo-YAP pathway in organ size control and tumorigenesis: an updated version. Genes Dev. *24*, 862–874. https://doi.org/10.1101/gad.1909210.

55. Zhao, B., Lei, Q.Y., and Guan, K.L. (2008). The Hippo-YAP pathway: new connections between regulation of organ size and cancer. Curr. Opin. Cell Biol. *20*, 638–646. https://doi.org/10.1016/j.ceb.2008.10.001.

56. Zanconato, F., Cordenonsi, M., and Piccolo, S. (2016). YAP/TAZ at the Roots of Cancer. Cancer Cell *29*, 783–803. https://doi.org/10.1016/j.ccell.2016.05.005.

57. Weil, J., Eschenhagen, T., Magnussen, O., Mittmann, C., Orthey, E., Scholz, H., Schäfer, H., and Scholtysik, G. (1997). Reduction of myocardial myoglobin in bovine dilated cardiomyopathy. J. Mol. Cell. Cardiol. *29*, 743–751. https://doi.org/10.1006/jmcc.1996.0318.

58. Heinke, M.Y., Wheeler, C.H., Yan, J.X., Amin, V., Chang, D., Einstein, R., Dunn, M.J., and dos Remedios, C.G. (1999). Changes in myocardial protein expression in pacing-induced canine heart failure. Electrophoresis *20*, 2086–2093. https://doi.org/10.1002/(sici)1522-2683(19990701)20:10<2086::Aid-elps2086>3.0.Co;2-4.

59. O'Brien, P.J., O'Grady, M., McCutcheon, L.J., Shen, H., Nowack, L., Horne, R.D., Mirsalimi, S.M., Julian, R.J., Grima, E.A., Moe, G.W., et al. (1992). Myocardial myoglobin deficiency in various animal models of congestive heart failure. J. Mol. Cell. Cardiol. *24*, 721–730. https://doi.org/10.1016/0022-2828(92)93386-x.

60. Branco, M.A., Cotovio, J.P., Rodrigues, C.A.V., Vaz, S.H., Fernandes, T.G., Moreira, L.M., Cabral, J.M.S., and Diogo, M.M. (2019). Transcriptomic analysis of 3D Cardiac Differentiation of Human Induced Pluripotent Stem Cells Reveals Faster Cardiomyocyte Maturation Compared to 2D Culture. Sci. Rep. *9*, 9229. https://doi.org/10.1038/s41598-019-45047-9.

61. Han, Z., Yu, Y., Cai, B., Xu, Z., Bao, Z., Zhang, Y., Bamba, D., Ma, W., Gao, X., Yuan, Y., et al. (2020). YAP/TEAD3 signal mediates cardiac lineage commitment of human-induced pluripotent stem cells. J. Cell. Physiol. *235*, 2753–2760. https://doi.org/10.1002/jcp.29179.

62. Neininger, A.C., Dai, X., Liu, Q., and Burnette, D.T. (2021). The Hippo pathway regulates density-dependent proliferation of iPSC-derived cardiac myocytes. Sci. Rep. *11*, 17759. https://doi.org/10.1038/s41598-021-97133-6.

63. Xin, M., Kim, Y., Sutherland, L.B., Murakami, M., Qi, X., McAnally, J., Porrello, E.R., Mahmoud, A.I., Tan, W., Shelton, J.M., et al. (2013). Hippo pathway effector Yap promotes cardiac regeneration. Proc. Natl. Acad. Sci. USA *110*, 13839–13844. https://doi.org/10.1073/pnas.1313192110.

64. Lin, Z., Zhou, P., von Gise, A., Gu, F., Ma, Q., Chen, J., Guo, H., van Gorp, P.R.R., Wang, D.Z., and Pu, W.T. (2015). Pi3kcb links Hippo-YAP and PI3K-AKT signaling pathways to promote cardiomyocyte proliferation and survival. Circ. Res. *116*, 35–45. https://doi.org/10.1161/circresaha.115.304457.

65. Li, J., Gao, E., Vite, A., Yi, R., Gomez, L., Goossens, S., van Roy, F., and Radice, G.L. (2015). Alpha-catenins control cardiomyocyte proliferation by regulating Yap activity. Circ. Res. *116*, 70–79. https://doi.org/10.1161/circresaha.116.304472.

66. Shao, D., Zhai, P., Del Re, D.P., Sciarretta, S., Yabuta, N., Nojima, H., Lim, D.S., Pan, D., and Sadoshima, J. (2014). A functional interaction between Hippo-YAP signalling and FoxO1 mediates the oxidative stress response. Nat. Commun. *5*, 3315. https://doi.org/10.1038/ncomms4315.

67. Kashihara, T., Mukai, R., Oka, S.I., Zhai, P., Nakada, Y., Yang, Z., Mizushima, W., Nakahara, T., Warren, J.S., Abdellatif, M., and Sadoshima, J. (2022). YAP mediates compensatory cardiac hypertrophy through aerobic glycolysis in response to pressure overload. J. Clin. Invest. *132*, e150595. https://doi.org/10.1172/jci150595.

68. Kashihara, T., and Sadoshima, J. (2019). Role of YAP/TAZ in Energy Metabolism in the Heart. J. Cardiovasc. Pharmacol. *74*, 483–490. https://doi.org/10.1097/fjc.0000000000000736.

69. Ikeda, S., Mukai, R., Mizushima, W., Zhai, P., Oka, S.I., Nakamura, M., Del Re, D.P., Sciarretta, S., Hsu, C.P., Shimokawa, H., and Sadoshima, J. (2019). Yes-Associated Protein (YAP) Facilitates Pressure Overload-Induced Dysfunction in the Diabetic Heart. JACC Basic Transl. Sci. *4*, 611–622. https://doi.org/10.1016/j.jacbts.2019.05.006.

70. Ikeda, S., Mizushima, W., Sciarretta, S., Abdellatif, M., Zhai, P., Mukai, R., Fefelova, N., Oka, S.I., Nakamura, M., Del Re, D.P., et al. (2019). Hippo Deficiency Leads to Cardiac Dysfunction Accompanied by Cardiomyocyte Dedifferentiation During Pressure Overload. Circ. Res. *124*, 292–305. https://doi.org/10.1161/circresaha.118.314048.

71. Wang, X., Senapati, S., Akinbote, A., Gnanasambandam, B., Park, P.S.H., and Senyo, S.E. (2020). Microenvironment stiffness requires decellularized cardiac extracellular matrix to promote heart regeneration in the neonatal mouse heart. Acta Biomater. *113*, 380–392. https://doi.org/10.1016/j.actbio.2020.06.032.

72. Mia, M.M., Cibi, D.M., Ghani, S.A.B.A., Singh, A., Tee, N., Sivakumar, V., Bogireddi, H., Cook, S.A., Mao, J., and Singh, M.K. (2022). Loss of Yap/taz in cardiac fibroblasts attenuates adverse remodeling and improves cardiac function. Cardiovasc. Res. *118*, 1785–1804. https://doi.org/10.1093/cvr/cvab205.

73. Bassat, E., Mutlak, Y.E., Genzelinakh, A., Shadrin, I.Y., Baruch Umansky, K., Yifa, O., Kain, D., Rajchman, D., Leach, J., Riabov Bassat, D., et al. (2017). The extracellular matrix protein agrin promotes heart regeneration in mice. Nature *547*, 179–184. https://doi.org/10.1038/nature22978.

74. Aharonov, A., Shakked, A., Umansky, K.B., Savidor, A., Genzelinakh, A., Kain, D., Lendengolts, D., Revach, O.Y., Morikawa, Y., Dong, J., et al. (2020). ERBB2 drives YAP activation and EMT-like processes during cardiac regeneration. Nat. Cell Biol. *22*, 1346–1356. https://doi.org/10.1038/s41556-020-00588-4.

75. Jue, T., Simond, G., Wright, T.J., Shih, L., Chung, Y., Sriram, R., Kreutzer, U., and Davis, R.W. (2016). Effect of fatty acid interaction on myoglobin oxygen affinity and triglyceride metabolism. J. Physiol. Biochem. *73*, 359–370. https://doi.org/10.1007/s13105-017-0559-z.

76. Hendgen-Cotta, U.B., Merx, M.W., Shiva, S., Schmitz, J., Becher, S., Klare, J.P., Steinhoff, H.J., Goedecke, A., Schrader, J., Gladwin, M.T., et al. (2008). Nitrite reductase activity of myoglobin regulates respiration and cellular viability in myocardial ischemia-reperfusion injury. Proc. Natl. Acad. Sci. USA *105*, 10256–10261. https://doi.org/10.1073/pnas.0801336105.

77. Götz, F.M., Hertel, M., and Gröschel-Stewart, U. (1994). Fatty acid binding of myoglobin depends on its oxygenation. Biol. Chem. Hoppe. Seyler. *375*, 387–392. https://doi.org/10.1515/bchm3.1994.375.6.387.

78. Flögel, U., Merx, M.W., Godecke, A., Decking, U.K., and Schrader, J. (2001). Myoglobin: A scavenger of bioactive NO. Proc. Natl. Acad. Sci. USA *98*, 735–740. https://doi.org/10.1073/pnas.011460298.

79. Flögel, U., Gödecke, A., Klotz, L.O., and Schrader, J. (2004). Role of myoglobin in the antioxidant defense of the heart. FASEB J. *18*, 1156–1158. https://doi.org/10.1096/fj.03-1382fje.

80. Chintapalli, S.V., Bhardwaj, G., Patel, R., Shah, N., Patterson, R.L., van Rossum, D.B., Anishkin, A., and Adams, S.H. (2015). Molecular dynamic simulations reveal the structural determinants of Fatty Acid binding to oxy-myoglobin. PLoS One *10*, e0128496. https://doi.org/10.1371/journal.pone.0128496.

81. Chintapalli, S.V., Anishkin, A., and Adams, S.H. (2018). Exploring the entry route of palmitic acid and palmitoylcarnitine into myoglobin. Arch. Biochem. Biophys. *655*, 56–66. https://doi.org/10.1016/j.abb.2018.07.024.

82. Wittenberg, J.B., and Wittenberg, B.A. (2003). Myoglobin function reassessed. J. Exp. Biol. *206*, 2011–2020. https://doi.org/10.1242/jeb.00243.

83. Shiva, S., Huang, Z., Grubina, R., Sun, J., Ringwood, L.A., MacArthur, P.H., Xu, X., Murphy, E., Darley-Usmar, V.M., and Gladwin, M.T. (2007). Deoxymyoglobin is a nitrite reductase that generates nitric oxide and regulates mitochondrial respiration. Circ. Res. *100*, 654–661. https://doi.org/10.1161/01.RES.0000260171.52224.6b.

84. Doeller, J.E., and Wittenberg, B.A. (1991). Myoglobin function and energy metabolism of isolated cardiac myocytes: effect of sodium nitrite. Am. J. Physiol. *261*, H53–H6262. https://doi.org/10.1152/ajpheart.1991.261.1.H53.

85. Li, F, Liu, R, Negi, V, Yang, P, Lee, J, Jagannathan, R, Moulik, M, Yechoor, VK, VGLL4 and MENIN function as TEAD1 corepressors to block pancreatic β cell proliferation. Cell Rep. 42(1):111904.

86. Yang, X., Zhang, M., Xie, B., Peng, Z., Manning, J.R., Zimmerman, R., Wang, Q., Wei, A.C., Khalifa, M., Reynolds, M., et al. (2023). Myocardial brain-derived neurotrophic factor regulates cardiac bioenergetics through the transcription factor Yin Yang 1. Cardiovasc. Res. *119*, 571–586. https://doi.org/10.1093/cvr/cvac096.

87. Branco, A.F., Pereira, S.P., Gonzalez, S., Gusev, O., Rizvanov, A.A., and Oliveira, P.J. (2015). Gene Expression Profiling of H9c2 Myoblast Differentiation towards a Cardiac-Like Phenotype. PLoS One *10*, e0129303. https://doi.org/10.1371/journal.pone.0129303.

88. Ménard, C., Pupier, S., Mornet, D., Kitzmann, M., Nargeot, J., and Lory, P. (1999). Modulation of L-type calcium channel expression during retinoic acid-induced differentiation of H9C2 cardiac cells. J. Biol. Chem. *274*, 29063–29070. https://doi.org/10.1074/jbc.274.41.29063.

89. Khoo, N.K.H., Rudolph, V., Cole, M.P., Golin-Bisello, F., Schopfer, F.J., Woodcock, S.R., Batthyany, C., and Freeman, B.A. (2010). Activation of vascular endothelial nitric oxide synthase and heme oxygenase-1 expression by electrophilic nitro-fatty acids. Free Radic. Biol. Med. *48*, 230–239. https://doi.org/10.1016/j.freeradbiomed.2009.10.046.

90. Cardenes, N., Corey, C., Geary, L., Jain, S., Zharikov, S., Barge, S., Novelli, E.M., and Shiva, S. (2014). Platelet bioenergetic screen in sickle cell patients reveals mitochondrial complex V inhibition, which contributes to platelet activation. Blood *123*, 2864–2872. https://doi.org/10.1182/blood-2013-09-529420.

91. Shiva, S., Sack, M.N., Greer, J.J., Duranski, M., Ringwood, L.A., Burwell, L., Wang, X., MacArthur, P.H., Shoja, A., Raghavachari, N., et al. (2007). Nitrite augments tolerance to ischemia/reperfusion injury via the modulation of mitochondrial electron transfer. JJ. Exp. Med. *204*, 2089–2102. https://doi.org/10.1084/jem.20070198.

92. Gentillon, C., Li, D., Duan, M., Yu, W.M., Preininger, M.K., Jha, R., Rampoldi, A., Saraf, A., Gibson, G.C., Qu, C.K., et al. (2019). Targeting HIF-1α in combination with PPARα activation and postnatal factors promotes the metabolic maturation of human induced pluripotent stem cell-derived cardiomyocytes. J. Mol. Cell. Cardiol. *132*, 120–135. https://doi.org/10.1016/j.yjmcc.2019.05.003.

93. Saraf, A., Rampoldi, A., Chao, M., Li, D., Armand, L., Hwang, H., Liu, R., Jha, R., Fu, H., Maxwell, J.T., and Xu, C. (2021). Functional and molecular effects of TNF-α on human iPSC-derived cardiomyocytes. Stem Cell Res. *52*, 102218. https://doi.org/10.1016/j.scr.2021.102218.

94. Hall, E.J., Pal, S., Glennon, M.S., Shridhar, P., Satterfield, S.L., Weber, B., Zhang, Q., Salama, G., Lal, H., and Becker, J.R. (2022). Cardiac natriuretic peptide deficiency sensitizes the heart to stress-induced ventricular arrhythmias via impaired CREB signalling. Cardiovasc. Res. *118*, 2124–2138. https://doi.org/10.1093/cvr/cvab257.

95. Yang, Q., Tang, Y., Imbrogno, K., Lu, A., Proto, J.D., Chen, A., Guo, F., Fu, F.H., Huard, J., and Wang, B. (2012). AAV-based shRNA silencing of NF-κB ameliorates muscle pathologies in mdx mice. Gene Ther. *19*, 1196–1204. https://doi.org/10.1038/gt.2011.207.

96. Satoh, T., Wang, L., Espinosa-Diez, C., Wang, B., Hahn, S.A., Noda, K., Rochon, E.R., Dent, M.R., Levine, A.R., Baust, J.J., et al. (2021). Metabolic Syndrome Mediates ROS-miR-193b-NFYA-Dependent Downregulation of Soluble Guanylate Cyclase and Contributes to Exercise-Induced Pulmonary Hypertension in Heart Failure With Preserved Ejection Fraction. Circulation *144*, 615–637. https://doi.org/10.1161/circulationaha.121.053889.

97. Gu, X., Matsumura, Y., Tang, Y., Roy, S., Hoff, R., Wang, B., and Wagner, W.R. (2017). Sustained viral gene delivery from a micro-fibrous, elastomeric cardiac patch to the ischemic rat heart. Biomaterials *133*, 132–143. https://doi.org/10.1016/j.biomaterials.2017.04.015.

98. Xin, C., Chu, X., Wei, W., Kuang, B., Wang, Y., Tang, Y., Chen, J., You, H., Li, C., and Wang, B. (2021). Combined gene therapy via VEGF and mini-dystrophin synergistically improves pathologies in temporalis muscle of dystrophin/utrophin double knockout mice. Hum. Mol. Genet. *30*, 1349–1359. https://doi.org/10.1093/hmg/ddab120.

99. Wang, B., Li, J., and Xiao, X. (2000). Adeno-associated virus vector carrying human minidystrophin genes effectively ameliorates muscular dystrophy in mdx mouse model. Proc Natl Acad Sci USA *97*, 13714–13719. https://doi.org/10.1073/pnas.240335297.

100. Rochon, E.R., Missinato, M.A., Xue, J., Tejero, J., Tsang, M., Gladwin, M.T., and Corti, P. (2020). Nitrite Improves Heart Regeneration in Zebrafish. Antioxid Redox Signal *32*, 363–377. https://doi.org/10.1089/ars.2018.7687.

101. Missinato, M.A., Saydmohammed, M., Zuppo, D.A., Rao, K.S., Opie, G.W., Kühn, B., and Tsang, M. (2018). Dusp6 attenuates Ras/MAPK signaling to limit zebrafish heart regeneration. Development *145*. https://doi.org/10.1242/dev.157206.

STAR★METHODS

KEY RESOURCES TABLE

REAGENT or RESOURCE	SOURCE	IDENTIFIER
Antibodies		
myoglobin	Santa Cruz Biotechnology	sc-393020, RRID:AB_2925016
LATS1	Cell Signaling Technologies	3477, RRID AB_2133513
pYAP	Cell Signaling Technologies	4911, RRID:AB_2218913
total YAP	Santa Cruz Biotechnology	271134, RRID:AB_10612397
alpha tubulin	Calbiochem	CP06, RRID:AB_2617116
Cardiac troponin	Thermo Fischer	MA5-12960, RRID:AB_11000742
myoglobin	biospacific	G-125-C, RRID:AB_2141816
actin	Abcam	ab8226, RRID:AB_306371
Sarcomeric actinin	Sigma Aldrich	A7811, RRID:AB_476766
H3P	Sigma	06-570, RRID:AB_310177
embCMHC	DSHB	N2.261, RRID:AB_531790
Mef2c	Santa Cruz Biotechnology	SC-313 RRID: AB_631920
PCNA	Sigma Aldrich	8825, RRID:AB_477413
Bacterial and virus strains		
AAV9 shRNA scramble control	University of Pittsburgh	This paper
AAV9 Mb shRNA	University of Pittsburgh	This paper
Catalase adenovirus	Vector biolabs	https://www.vectorbiolabs.com/product/1475-catalase-adenovirus/
Empty vector adenovirus	Vector biolabs	https://www.vectorbiolabs.com/product/1240-adenovirus-null-adenovirus/
Chemicals, peptides, and recombinant proteins		
YAP peptide	abnova	H00010413-P01
LATS1	abcam	ab125612
Donkey serum	Sigma	d9663
B27	Gibco	17504044
Critical commercial assays		
ON-TARGETplus Mb siRNA	Dharmacon	L-094211-02-0005
Control siRNA	Dharmacon	D-001810-01-05
Transit-X2 transfection reagent	Mirus	MIR6004
Mouse Mb siRNA	Santa cruz	sc-35994
Control siRNA	Santa cruz	sc-37007
SYBR master mix	Thermo	A25742
Amplex red	Thermos fischer	A22177
oxyblot	EMD millipore	S7150
ADP glo kinase assay	Promega	V6930
RNA isolation	Qiagen	74134
cDNA synthesis	biorad	1708891
Experimental models: Cell lines		
H9C2	ATCC	https://www.atcc.org/products/crl-1446
HL-1	Sigma	https://www.sigmaaldrich.com/US/en/product/mm/scc065
iPSC	NIH	https://commonfund.nih.gov/stemcells/lines

(*Continued on next page*)

Continued

REAGENT or RESOURCE	SOURCE	IDENTIFIER
Experimental models: Organisms/strains		
Primary cardiomyocytes	Envigo	https://www.inotivco.com/model/hsd-sprague-dawley-sd
Zebrafish myoglobin knockout	University of Pittsburgh	This paper
Wildtype mice	Jackson labs	https://www.jax.org/strain/000664, RRID:IMSR_JAX:000664
Recombinant DNA		
Myoglobin plasmid	origene	https://www.origene.com/catalog/cdna-clones/expression-plasmids/rg212352/myoglobin-mb-nm_005368-human-tagged-orf-clone
Apo myoglobin	University of Pittsburgh	Braganza et al.[36]
TEAD reporter	University of Pittsburgh (Dr. Moulik)	Li et al.[85]
YAP S3D	Lab of Dr. Jixin Dong	Yang et al.[34]
rAAV9 plasmid	University of Pittsburgh	This paper
Software and algorithms		
PRISM 9.5.1	Graphpad	https://www.graphpad.com/
NIS elements	Nikon	https://www.microscope.healthcare.nikon.com/products/software/nis-elements
Image Studio Lite Ver 5.2	LI-COR Biosciences	https://www.licor.com/bio/image-studio/
Plasmid sequencing provider	Plasmidsaurus	https://www.plasmidsaurus.com/

RESOURCE AVAILABILITY

Lead contact

Further information and requests for resources and reagents should be directed to the lead contact, Dr. Sruti Shiva (sss43@pitt.edu).

Materials availability

Reagents generated in this study including AAV9 and CRISPR-Cas9 zebrafish knockout lines are available upon request from the lead contact with a completed Materials Transfer Agreement.

Data and code availability

All data reported in this paper will be shared by the lead contact upon request. This paper does not report original code.

EXPERIMENTAL MODEL AND STUDY PARTICIPANT DETAILS

Animal studies

All studies and procedures involving animals were approved by the University of Pittsburgh Animal Care and Use Committees (Institutional Animal Care and Use Committee (IACUC)) in accordance with National Institutes of Health guidelines. Mice were housed in standard facilities maintained at 21–23°C with 5–70% humidity, 12 h dark-light cycle in a pathogen-free facility, with *ad libitum* access to food and water. AAV9 injections were performed in one-day-old neonatal C57Bl6/J mice obtained from purchasing pregnant dams at E13-16-week gestation. Neonatal rat cardiomyocytes were isolated from pups born from pregnant Sprague-Dawley rats (gestational age 18 days) were purchased from Envigo. Zebrafish were maintained and used for myocardial injury experiments according to standard protocols approved by the University of Pittsburgh's IACUC, conforming to NIH guidelines.

Cell lines

H9C2 cells were purchased from ATCC and HL-1 cells were purchased from Sigma. H9C2 cells were cultured in DMEM media containing high glucose, pyruvate 10% fetal bovine serum and antibiotics while HL-1 cells were cultured in Claycomb medium supplemented with fetal bovine serum and antibiotics. All cells were cultured at 37°C at 5% CO2 under sterile conditions. ND2.0 NIH CRM control iPSCs were obtained from the NIH and cultured according to established guidelines.

Primary cell cultures Neonatal Sprague-Dawley rat myocytes were isolated from 1 to 3 days old neonate hearts, and the sex of neonates was not observable at that time point. All cells from the neonatal hearts were pooled for experiments. Cells were cultured in DMEM (with high glucose and pyruvate, Invitrogen Cat # 11995073) with 10% FBS for the first day, and then FBS was replaced by insulin-Transferrin-Selenium (ITS, Thermal Fisher Cat # 41400045) the next day. Cells were cultured at 37 $\pm$ 0.5°C with 5% CO2.

METHOD DETAILS

Neonatal rat cardiomyocyte isolation

All procedures involving murine models were approved by the University of Pittsburgh's IACUC in accordance with National Institutes of Health guidelines. As previously described,[86] hearts from 1–2-day old Sprague-Dawley rat pups were excised into cold buffer (NaCl 137 mM, KC1 5.36 mM, MgSO4–7H2O 0.81 mM, dextrose 5.55 mM, KH2PO4 0.44 mM, Na2HPO4–7H2O 0.34 mM, and HEPES 20 mM at pH 7.5). Ventricles were cleared of blood and dissected into 1–2 mm pieces to digest out cardiomyocytes using multiple incubations in trypsin (0.04%) and collagenase (0.4 mg/mL) at 37°C on a rocking platform. Cardiomyocytes were then purified from the fibroblasts by pre-plating for 90 min and were plated on Matrigel or 0.1% gelatin coated culture dishes prior to performing knockdown studies. Cells were cultured in serum free DMEM containing 0.1% Insulin-transferrin-selenium (Thermo Fisher Scientific).[86] Data are from 3 biological replicates, i.e., 3 separate litters.

Cell culture

H9C2 undifferentiated rat myoblasts were purchased from ATCC and maintained in 10% FBS supplemented with antibiotics and L-glutamine. HL-1 cells were obtained from Sigma and cultured in Claycomb medium supplemented with 10% FBS. H9C2 cells were stimulated to differentiate when cells were at 70–80% confluence using 1% serum medium supplemented with 10 nM Retinoic acid and maintained in differentiation media for 5 days as described.[87,88]

Myoglobin knockdown

Transient knockdown of myoglobin in H9C2 rat cells and primary neonatal rat ventricular myocytes was performed using ON-TARGETplus Rat Mb siRNA (L-094211-02-0005, Dharmacon) or control non-targeting siRNAs (D-001810-01-05, Dharmacon; 50 nM). Cells were grown to 70% confluency and siRNAs were transfected with Mirus TransIT-X2 (MIR6004, Mirus Bio) following manufacturer instructions in OPTI-MEM medium (31985070, Thermo Fisher). Cells were analyzed at 48 h post transfection. Transient knockdown in mouse HL-1 cells was performed with siRNA particles targeted to mouse myoglobin (sc-35994, Santa Cruz) or non-targeting scramble siRNA (sc-37007, Santa Cruz) following the same protocol. For all cell culture experiments with H9C2 and HL-1 cells, N is the number of biological replicates and includes cells from distinct passages.

Proliferation

Cells were plated in 96 well cell culture plates at a density of 5000 cells/well. 48 h later, cells were fixed and stained with crystal violet (0.2%w/v, 30 min), resolubilized in 1% SDS, and absorbance was measured at 595 nm.

PCR

RNA was extracted using RNAeasy spin columns (#74134, Qiagen) according to manufacturer instructions. Equal concentration of mRNA was measured and used as template for first strand DNA synthesis (#1708891, Biorad). The cDNA was used as input in quantitative RT-PCR reactions using PowerUp SYBR Green Master Mix (A25742, Thermo Fisher). All primers were obtained from integrated DNA Technologies and sequences are 5′-3′.

Rat primers: mlc-2vF (AGGCCTTCACAATCATGGAC), mlc-2vR (TCGTTTTTC ACGTTCACTCG), myh6F(GCCTACCTCATGGGACTGAA), myh6R (ACATTCTGC CCTTTGGTGAC), tnnt2F(CCTGCAGGAAAAGTTCAAGC), tnnt2R (GTGCCTGGCAAGACCTAGAG), 18SF (TTGATTA AGTCCCTGCCCTTTGT), 18SR (CGATCCGAGGGCCTAACTA), calseqF (TCA AAG ACC CAC CCT ACG TC), calseqR (GAG GAA AGT CGT CTG GGT CA), plnF (ACC TTA CTC GCT CGG CTA TC), plnR (GTT GTA AGC TGA CGT TGG CA), ryr2F (CCC ACC TCC TTG ACA TCG), ryr2R (CCC ACC TCC TTG ACA TCG). Mouse primers: tnnt2F(CAGAGGAGGCCAACGTAGAAG), tnnt2R (CTCCATCGGGGATCTTGGGT), Human primers: actinF (ATTACGCTGCGTTCTCTTC), actinR (CTGATGGGATGAGTGATTACAG), tnnt2F(TTCACCAAAGATCTGCTCCTCGCT), tnnt2R (TTATTACTGGTGTGGAGTGGGTGT), myh6F(TCAGCTGGAGGCCAAAGTAAAGGA), myh6R (TTCTTGAGCTCTGAGCACTCG TCT), ryr2F (TAGATTTATAAGGGGCCTTG), ryr2R (GATTCTTCAGGGCT GTAGT).

Western blot

Mouse tissue lysates were prepared in RIPA lysis buffer (89900 Thermo Fischer) containing protease and phosphatase inhibitors using a bead homogenizer (mini bead mill). Cell lysates were prepared using cOmplete Lysis-M (4719956001, Roche) with protease and phosphatase inhibitors and subjected to standard electrophoresis and transfer as previously described.[89] Following transfer, membranes were blocked, incubated in primary antibody (overnight, 4C) followed by incubation in species specific secondary antibody (1:10,000 Li-COR; 2 h; room temperature) before imaging on an Odyssey CLx (Li-COR Biosciences). The primary antibodies include pYAP (1:500, 4911, Cell Signaling Technologies), T-YAP (1:1000, H-9, sc-271134 Santa Cruz), Mb (1:1000, LS-C144978 LS Bio or 1:1000, sc-393020 Santa Cruz), Tubulin (1:1000, CP06, Calbiochem), 1:2500 beta-actin (ab8226, Abcam).

Hydrogen peroxide measurement

200,000 cardiomyocytes were incubated in Amplex Red (5 μM; 2 min) for cellular H2O2 (A22177, ThermoFisher). The rate of production was calculated by measuring the linear phase of the kinetic fluorescence emission curves (571/585 nm: Amplex red) over 30 min as previously described.[90,91]

TEAD reporter activity

TEAD reporter plasmid was transfected into H9C2 being treated with control or Mb specific siRNA using Mirus TransIT-X2 (MIR6004, Mirus Bio) according to manufacturer instructions. 10,000 cells per well were analyzed 48 h after reporter transfection by luminescence measurements using a commercial luciferase assay system (E1500, Promega) according to recommended manufacturer protocol. The assay was repeated in 3 sets of independent knockdowns with atleast 2 sets of TEAD reporter transfections.

LATS1 kinase activity and oxidation

LATS1 kinase activity was measured in assay was performed in recombinant LATS1 (2 ng) or LATS1 immunoprecipitated from cell lysates using an antibody specific to LATS1 (4 μg; CST:3477). Immunoprecipitated LATS1 was incubated with YAP peptide (1 μg) and ATP (10 μM). After completion of the reaction (30°C; 30 min), the kinase mix was incubated with ADP-Glo reagent (40 min) and luminescence resulting from ADP conversion to ATP was measured following the manufacturer's instructions (Promega; ADP-Glo Kinase Assay, V6930). To measure changes in oxidation, LATS1 kinase was immunoprecipitated from 500 μg of protein lysates and subject to Oxyblot assay (#S7150, Millipore) according to manufacturer's instructions.

Cell immunofluorescence

Cells were cultured on chamber slides (Millipore C7182-1PAK), fixed in 4% formaldehyde (Thermo 50-980-487; 12 min, 20°C) and then blocked with 5% normal donkey serum (Sigma-Aldrich D9663; 30 min) and Triton X-100 (0.01% in PBS). This followed by incubation in primary antibodies to H3P (1:500; 06–570, Sigma), alpha-sarcomeric actinin (1:500; A7811, Sigma), cardiac troponin (1:500; MA5-12960, Thermo Fisher) and total-YAP (1:250, sc-101199, Santa Cruz) overnight at 4°C. Cells were then washed in PBS (3 times for 5 min) and incubated at room temperature in Alexa Fluor conjugated secondary antibodies (1 h; 1:500; A-21206, R37115, Thermo Scientific). Cells were washed in PBS (3 times for 5 min) prior to nuclear counterstaining with DAPI in mounting media (Vector BioLabs). For measurements of dedifferentiation in isolated cardiomyocytes, lengths of troponin filaments were measured using the length measurement tool on NIS elements analysis software. Data are represented as fold change from 3 separate isolations.

iPSC differentiation

iPSC cells were seeded in a 6-well growth-factor-reduced Matrigel coated plate. Cells reached a confluency of 70–80% prior to initiation of differentiation. At the start of differentiation, RPMI B27 minus supplemented with GSK3 inhibitor CHIR (6 μm) was added to the cells for 2 days, following which medium was replaced with 2 mL of fresh RPMI B27 minus for one day. On day 3, medium fresh RPMI B27 minus differentiation media supplemented with 5 μM WNT inhibitor IWR-1 was added to the cells. On Day 5 media was changed to RPMI B27 minus for 2 days at which point on day 7 RPMI with B27 supplement was added after removing the older RPMI B27- media. On day 9, at which point there was observable cardiomyocyte contractility, media was changed to RPMI 1640 without glucose containing B27 supplement. On day 11 and following that, cells were maintained in RPMI B27 with media changes every 2 days. At day 12, either siRNA targeting scramble control or human Mb were added to cells at 50 nM final concentration with Mirus TransIT-X2. siRNA was replenished every 48 h till qPCR analysis for marker genes at day 18.[92–94] This differentiation protocol yields >90% cardiomyocytes.

Construction of the mouse myoglobin shRNA, AAV9 production and injection

The scramble non-targeting shRNA cassette or Mb specific shRNA sequence were cloned into a rAAV9 vector under the control of the human U6 promoter, followed by a ZsGreen expression cassette driven by CMV promoter to serve as a marker to monitor the shRNA delivery efficiency *in vivo*. Complementary double stranded control or Mb targeting shRNA oligos were generated with *BamH* I/*EcoR* I stick ends by annealing for 5 min at 95°C followed by a slow decrease in temperature ramp from 95°C up to 25°C and overnight at 4°C. The sticky ended oligos shRNA were cloned into the same restriction enzyme sites of rAAV vector that was pre-treated by double-digestion. Control and Mb-specific shRNA in the AAV construct were fully sequenced at Plasmidsauraus (https://www.plasmidsaurus.com/). rAAV9 viruses were generated by triple plasmid co-transfection of 293 cells and purified twice with cesium chloride gradient ultracentrifugation according to a previously published protocols.[95–98] The vector titers were determined by the DNA dot blot to be $7 \times 10^{12} - 1 \times 10^{13}$ viral genome copies per mL (v.g./mL).[99] 10 mL of purified AAV9 particles were injected into the thoracic cavity of postnatal day 1 old C56Bl6/J, followed by analysis at postnatal day 7.

Zebrafish myocardial amputation model: Adult zebrafish (D. rerio) were maintained according to standard protocols

Husbandry protocols and experiments were approved by the IACUC at the University of Pittsburgh, which conforms to guidelines set by the NIH. A 37-base pair (bp) genomic insertion resulted from a non-homologous end-joining repair error following injection of a sgRNA targeting the first exon of zebrafish *mb* using CRISP-Cas9 genome editing. Target site GGATCTGGTTCTGAAGTGCTG (pt813) was selected using CHOPCHOP

software. The sgRNA was made according to recommended protocol, using the Megashort SP6 Transcription kit (ThermoFisher, AM1330) followed by RNA purification with the Megaclear Kit (ThermoFisher, AM1908). *Cas9* mRNA was synthesized from pCS2-nCas9 n using the mMessage mMachine SP6 Transcription kit (ThermoFisher, AM1340). Approximately 2 nL of the RNA mixture of sgRNA (500 pg) and Cas9 mRNA (600 pg) were coinjected at 1 cell stage. Embryos were raised and screened for changes in PCR amplicon size (mutants being 37 bps longer) using primers specific to exon 1 of *mb* (forward primer: 5′- GCACATCCATACATCGCTTG-3′, reverse 5′– GACAATAATCGAGCAGCCTTAGA–3′). To induce cardiac regeneration, age matched adult wt and *mb−/−* zebrafish were anesthetized for 3–5 min in ethyl 3-aminobenzoate methanesulfonate salt (0.168 g/dL). A small incision was made on the ventral wall to access the heart and approximately 20% of the heart ventricle was amputated using a pair of sterile fine scissors, following which fish were allowed to recover in water for 30 min and then returned to the tank until the time of assays.[100,101] For zebrafish Western blots, N represents 3 independent batches of zebrafish lysate, each prepared from pooling lysates from 5 to 6 fish ventricles.

Histology, immunofluorescence and imaging of zebrafish and mice hearts

Hearts were collected from sedated zebrafish, washed in cold PBS, and fixed in 4% paraformaldehyde. The hearts were then cryopreserved in a sucrose gradient and embedded in Surgipath Cryo-Gel (Leica). Ten to twelve micrometer cryosections were prepared and consecutive sections were used for AFOG staining or immunofluorescence. The injured area of the zebrafish heart was measured and averaged from the 3 sections displaying the largest injured area in each heart. The primary antibodies used for immunostaining were anti-embCMHC (N2.261, 1:50, DSHB), anti-Mef2C (SC-313, 1:500; Santa Cruz Biotechnology), anti-PCNA (8825, 1:1000; Sigma). The secondary antibodies used for immunostaining (1:1000; Thermo Fisher) were goat-*anti*-rabbit Alexa Fluor 488 (A11008), goat-*anti*-rabbit Alexa Fluor Cy3 (A10520), goat-*anti*-mouse Alexa Fluor Cy3 (A10521), and goat-*anti*-mouse Alexa Fluor 488 (A11001). Slides were stained with DAPI (1:1000; Thermo Fisher), followed by treatment with Vectashield mounting medium (Vector Laboratories). Confocal images were taken with a Zeiss LSM 200 confocal microscope. Two-dimensional projections were generated from z series (1 μm steps). Mef2C/Pcna double-positive cells were manually counted over three separate consecutive sections, averaged, and normalized to the total area counted. Only hearts that had a clear injury located in the center sections of the heart were considered for each experiment. Mouse hearts were harvested after decapitation and hears were washed in PBS followed by fixation for 2 h at RT in 4% PFA. Fixed hearts were cryoprotected after 30% sucrose equilibration and mounted with OCT (Tissue-Tek) for preparing 10-micron sections. Sections were blocked in 5% donkey serum, stained with antibody to phosphohistone 3 (1:500; 06–570, Sigma) overnight at 4C followed by 3 washes in tween-TBS and secondary antibody incubation (donkey anti-rabbit 1: 500, Alexa 547) in PBS at RT for 1 h. Slides were mounted with Vectashield mounting medium containing PBS and imaged with a 20× objective on a Nikon A1-R confocal (Center for Biologic Imaging, University of Pittsburgh). N represents biological replicates and includes at least 3 sections per mouse with 4 images captured per mouse.

QUANTIFICATION AND STATISTICAL ANALYSIS

All bar graphs depict mean ± SEM. Statistical analysis was performed using Graphpad Prism 9 software. Two groups were compared for statistical significance using a two-tailed Student's *t* test. ANOVA with post-hoc testing was used to make multiple comparisons of more than 2 groups. Differences were considered statistically significant when $p < 0.05$.